High-Pressure Synthesis, Crystal Structure and Properties of GdS2 with Thermodynamic Investigations in the Phase Diagram Gd - S

Carola J. Müller, Ulrich Schwarz, Peer Schmidt, Walter Schnelle, Thomas Doert

Zeitschrift für Anorganische und Allgemeine Chemie

High-Pressure Synthesis, Crystal Structure and Properties of GdS2 with Thermodynamic Investigations in the Phase Diagram Gd – S

Journal:	*Zeitschrift für Anorganische und Allgemeine Chemie*
Manuscript ID:	zaac.201000015.R1
Wiley - Manuscript type:	Article
Date Submitted by the Author:	19-Feb-2010
Complete List of Authors:	Müller, Carola J.; Max-Planck-Institut für Chemische Physik fester Stoffe Schwarz, Ulrich; Max-Planck-Institut für Chemische Physik fester Stoffe Schmidt, Peer; Technische Universität Dresden, Fachrichtung Chemie und Lebensmittelchemie Schnelle, Walter; Max-Planck-Institut für Chemische Physik fester Stoffe Doert, Thomas; Technische Universität Dresden, Fachrichtung Chemie und Lebensmittelchemie
Keywords:	Polysulfides, gadolinium, high-pressure synthesis, crystal structure, phase diagram

ARTICLE

DOI: 10.1002/zaac.200((will be filled in by the editorial staff))

High-Pressure Synthesis, Crystal Structure and Properties of GdS_2 with Thermodynamic Investigations in the Phase Diagram Gd – S

Carola J. Müller[a,b], Ulrich Schwarz[b], Peer Schmidt[a], Walter Schnelle[b] and Thomas Doert[a]*

Dedicated to Prof. Dr. Rüdiger Kniep on the Occasion of his 65th Birthday

Keywords: Polysulfides; gadolinium; high-pressure synthesis; crystal structure; phase diagram

Gadolinium disulfide has been prepared by high-pressure synthesis at 8 GPa and 1173 K. It crystallizes in the monoclinic space group $P12_1/a1$ (No. 14) with lattice parameters $a = 7.879(1)$ Å; $b = 3.936(1)$ Å, $c = 7.926(1)$ Å and $\beta = 90.08(1)°$. The crystal structure is a twofold superstructure of the aristotype ZrSSi and consists of puckered cationic $[GdS]^+$ double slabs which are sandwiched by planar sulfur sheets containing S_2^{2-} dumbbells. The thermal decomposition of GdS_2 proceeds via the sulfur-deficient polysulfides $GdS_{1.9}$, $GdS_{1.85}$ and $GdS_{1.77}$ and eventually results in the sesquisulfide Gd_2S_3.
GdS_2 is a paramagnetic semiconductor which orders antiferromagnetically at $T_N = 7.7(1)$ K. A metamagnetic transition is observed in the magnetically ordered state.

[a] Fachrichtung Chemie und Lebensmittelchemie, Technische Universität Dresden, Helmholtzstr. 10, 01062 Dresden
Fax: + 351 463 37287
E-mail: thomas.doert@chemie.tu-dresden.de
[b] Max-Planck-Institut für Chemische Physik fester Stoffe, Nöthnitzer Str. 40, 01187 Dresden

Introduction

Polychalcogenides of rare-earth elements are known since 1908 when *Biltz* synthesized CeS_2 [1]. The crystal structures of the polysulfides $LnX_{2-\delta}$ (Ln = Y, La, Ce – Lu; X = S, Se; $0 \le \delta \le \approx 0.2$) of the trivalent rare-earth metals contain puckered double slabs $[Ln^{3+}X^{2-}]$ which are sandwiched by planar chalcogen layers $[X^{\delta-}]$. The same atomic pattern is also found in the ZrSSi type which thus can be considered as the aristotype for these rare-earth metal polychalcogenides. The differences in the chalcogen content of theses compounds severely affect the electronic structure and the arrangement of the atoms in the planar layers. The number of chalcogen defects and their ordering pattern determine which kind of superstructure is formed. In recent years considerable efforts have been made to understand the phase relations between polychalcogenides of different composition and to determine their closely related superstructures (cf. [2 – 7]).

Two crystalline modifications for stoichiometric compounds LnS_2 and $LnSe_2$ have been characterized. The monoclinic α-modification (also called $CeSe_2$ type, $P12_1/a1$, $Z = 4$) is adopted by the disulfides and diselenides from lanthanum to neodymium. [2, 6, 8] The polytypic orthorhombic β-modification (space group $Pnma$, $Z = 8$) is known for the disulfides from lanthanum to neodymium [6, 9]. Chalcogen-poorer compounds of the formula type $LnX_{1.9}$ crystallize in the $CeSe_{1.9}$ type (space group $P4_2/n$, $Z = 20$). This structural pattern is formed for polysulfides $LnS_{1.9}$ with Ln = La – Nd, Sm and Gd and for polyselenides $LnSe_{1.9}$ with Ln = La – Nd and Sm [3, 10]. For yttrium and the smaller lanthanide metals (terbium – lutetium) only compounds with higher chalcogen deficiency like $LnX_{1.875}$ or $LnX_{1.85}$ (Ln = Y, Gd – Er, X = S, Se) have been synthesized [4, 5, 7, 11].

Thermoanalytical and tensimetric studies reveal that polysulfides and polyselenides $LnX_{2-\delta}$ generally decompose at elevated temperatures by a stepwise release of molecular chalcogen X_2 until the sesquichalcogenide Ln_2X_3 is finally reached [4, 12]. Polychalcogenides of the smaller rare-earth metals have a higher decomposition pressure which is the reason that all attempts to synthesize stoichiometric disulfides or diselenides of those metals failed up to now. The increasing decomposition tendency with decreasing lattice parameters of the polychalcogenides is mainly attributed to growing anti-bonding interactions between the chalcogenide anions in the planar layers.

High-pressure synthesis is one tool to directly counteract the decomposition of rare-earth metal dichalcogenides $LnX_{2.0}$ to chalcogen defect polychalcogenides $LnX_{2-\delta}$. Earlier, *Webb* and *Hall* have prepared compounds $LnX_{2-\delta}$ by high-pressure synthesis in a pressure range from 1 to 7 GPa and temperatures up to 1700 K [13]. They reported a pseudotetragonal and a pseudocubic modification of the lanthanide disulfides LnS_2 (Ln = Gd – Lu) and a pseudotetragonal modification of the lanthanide diselenides $LnSe_2$ (Ln = Er – Lu). However, structure determinations on the basis of single crystal data and chemical analyses of the reaction products are missing. Later, *Yanagisawa et al.* succeeded to grow single crystals of β-CeS_2 under high-pressure conditions [9]. They also observed evidence for a phase transition from the monoclinic to the orthorhombic modification at $p > 5.5$ GPa for the compounds PrS_2 and NdS_2. Raman spectroscopic investigations up to 16 GPa at 293 K could not validate these results for the lanthanide disulfides with Ln = La – Nd [14]. Recently, *Schleid et al.* synthesized the orthorhombic modification of the disulfides LnS_2 of La, Ce and Pr at ambient pressure [6].

In this work we present the first results of high-pressure studies on rare-earth metal polysulfides. In this contribution we focus on the synthesis of GdS_2, its crystal structure and some physical properties as well as on thermodynamic investigations in the binary system gadolinium – sulfur.

Results and Discussion

Synthesis

In order to find suitable conditions for formation and crystal growth of GdS_2 several reaction routes were tested at high-pressure conditions:

$$Gd + 2\ S \rightarrow GdS_2, \quad (1)$$

$$GdS_{1.9} + 0.1\ S \rightarrow GdS_2, \quad (2)$$

$$Gd_2S_3 + S \rightarrow 2\ GdS_2 \quad (3)$$

and

$$2\ GdCl_3 + 3\ K_2S_2 \rightarrow 2\ GdS_2 + 6\ KCl + 2\ S. \quad (4)$$

A slight excess of sulfur has been used, namely starting ratios Gd : S of 1 : 2.2, for all reaction routes to avoid the formation of chalcogen deficient polysulfides $GdS_{2-\delta}$ with $\delta > 0$. Besides the reaction route (i. e. the starting material) temperature, pressure and reaction time were varied in the experiments. The target compound GdS_2 is obtained at 8 GPa, 1173 K and 3 h annealing time from any of the selected reactions, see equations (1) – (4). The excess of sulfur could not be detected in the powder X-ray diffraction patterns of the reaction products; it was most probably obtained as an amorphous phase. At a pressure of 3 GPa and a similar induction heating and annealing program only $GdS_{1.9}$ was obtained. At $p = 15$ GPa and a temperature of 1173 K GdS_2 was yielded as a by-product to Gd_2S_3. Interestingly GdS_2 does also form at ambient temperature if a pressure of 8 GPa is applied for 50 h.

The optimization of the temperature program was done with mixtures of gadolinium sesquisulfide and sulfur at 8 GPa. Different reaction temperatures between 1373 K and 1823 K (induction heating period, usually held for 15 min) followed by different annealing steps (1173 K – 1573 K, for 3 h – 43 h) were tested. The sample from which the crystal for the X-ray structure determination was taken was heated to 1373 K in 15 min, kept at this temperature for another 15 min and subsequently cooled to 1173 K during 2 h. This temperature was then kept for 15 h.

For reaction path (4) the alkali-metal halide can be removed by leaching with a mixture of water and ethanol but the excess sulfur still remains in the product. Adding the flux material in ratios GdS_2 : CsCl of 1 : 6 and 6 : 1 or changing the element ratio of Gd : S to 1 : 3 or even 1 : 6 did not improve the crystal quality of the samples.

In short, according to the powder X-ray diffraction diagrams of the reaction products pure polycrystalline α-GdS_2 could be obtained from routes (1), (2) and (3) at $p \geq 8$ GPa and 973 K $\leq T \leq$ 1573 K. During our investigations, we found no evidence for polysulfides with higher sulfur content than GdS_2 or for a phase transition of monoclinic α-GdS_2 to the orthorhombic β-modification.

The reflections in the X-ray diffraction patterns of crystalline powders synthesized in different batches exhibit strongly varying full widths at half maximum and signal/background ratios. This result is taken as an indication for marked differences in the size of the crystalline domains of various batches. Powder patterns indicating poor quality were obtained from products prepared according to the route of *Webb* and *Hall* (1) starting from the elements [13]. The solid state metathesis reaction (4) results in diffraction patterns of better quality but due to the small content of target material and the large amount of by-products this method was not considered for further experiments. The quality of samples synthesized from gadolinium sesquisulfide (2) or gadolinium polysulfide $GdS_{1.9}$ (3) is similar. Since the synthesis of $GdS_{1.9}$ is more difficult and time-consuming than that of Gd_2S_3, all subsequent high-pressure experiments were performed starting from mixtures of gadolinium sesquisulfide and sulfur.

The domain size of the reaction products could be increased by annealing the samples in the temperature range of the sulfur melt at 8 GPa. This effect is attributed to an enhanced diffusion in the solid phase at high annealing temperatures which accelerates the growth of the grains. The effect that during the cooling phase bigger seed crystals grow at the expense of smaller ones is the well-known *Ostwald* ripening. When the temperature exceeds about 1700 K gadolinium disulfide decomposes to gadolinium polysulfide $GdS_{1.9}$, gadolinium sesquisulfide Gd_2S_3 and sulfur.

Chemical Analysis

The carrier gas hot extraction method did not evidence oxygen, nitrogen or hydrogen in the analyzed sample. The EDXS analysis on different parts of a sample resulted in a composition Gd : S of 1 : 1.97(2) confirmed in good agreement with the assumed composition GdS_2.

Crystal Structure

The results of the crystal structure analysis reveal that GdS_2 adopts the CeS_2 (or α-LnS_2) type. It crystallizes in the monoclinic space group $P12_1/a1$ (No. 14). The cell parameters are $a = 7.879(1)$ Å, $b = 3.936(1)$ Å, $c = 7.926(1)$ Å and $\beta = 90.08(2)°$. The results of the crystal structure refinement and selected interatomic distances are listed in tables 1–3.[1]

As has been discussed, the atomic pattern consists of puckered cationic $[GdS]^+$ double slabs of Gd^{3+} and S^{2-} ions (S1 in tables 2 and 3). These double slabs, which can more precisely be described with the *Niggli* formula ${}^2_\infty[GdS_{5/5}]^+$, are sandwiched by planar layers containing S_2^{2-} dimers accordingly. Four S atoms of three different S_2^{2-} anions complete the Gd coordination polyhedron, a capped slightly distorted quadratic antiprism.

[1] Further details concerning the structure analysis can be obtained from the Fachinformationszentrum Karlsruhe, 76344 Eggenstein-Leopoldshafen, quoting the depository number CSD-421335.

Table 1: Crystallographic data and refinement parameters of GdS_2.

chemical composition	GdS_2
M_r, g/mol; $F(000)$	221.37; 384
temperature, K	296(2)
diffractometer type	Kappa CCD (Bruker-AXS)
wavelength, Å	0.71073 (Mo Kα, graphite monochromator)
crystal system	monoclinic
space group (No.); Z	$P12_1/a1$ (14); 4
cell parameters	a = 7.879(1) Å, b = 3.936(1) Å
(single crystal data)	c = 7.926(1) Å, β = 90.08(1)°
cell volume, Å^3	245.8(1)
density, g/cm^3	5.98
absorption coefficient, mm^{-1}	28.3
absorption correction	multi-scan (*SADABS*, [15])
T_{min} / T_{max}	0.2355 / 0.4650
crystal size, mm^3	0.036 × 0.021 × 0.004
measurement range	$2.57 < \Theta < 35.02$
	$-12 \le h, l \le 12$
	$-6 \le k \le 6$
N(meas); N(unique); N(obs)	6223; 1505; 1396
R_{int}	0.025
refinement method	full-matrix least squares on F^2, *JANA2006* [16]
restrictions / parameters	0 / 31
goodness-of-fit on F^2	1.02
R_1;ωR_2 (reflections $I > 3\sigma(I)$)	0.018; 0.040
R_1;ωR_2 (all reflections)	0.021; 0.041
$\Delta\rho_{min}$ / $\Delta\rho_{max}$, eÅ^{-3}	–1.00 / 0.95
twin matrices	(0 –0.5 0, 2 0 0, 0 0 1)
	(–1 0 0, 0 –1 0, 0 0 1)
	(0 0.5 0, –2 0 0, 0 0 1)
twin volume ratios	0.076(4), 0.076(2),
	0.638(2), 0.210(2)

Insert Figure 1 here

Table 2: Fractional coordinates and isotropic displacement parameters of GdS_2.

Atom	x	y	z	U_{eq}, Å^2
Gd	0.12938(3)	0.78670(7)	0.72427(2)	0.00744(4)
S1	0.1251(1)	0.7609(2)	0.3674(1)	0.0078(2)
S2	0.1097(1)	0.3399(2)	–0.0031(1)	0.0088(2)

As stated above, the crystal structure of monoclinic GdS_2 (CeS_2 type) can be derived from the tetragonal ZrSSi type structure. The symmetry reduction is required due to the formation of disulfide anions in the planar chalcogen layers. The *Bärnighausen* tree for the three-step symmetry reduction to maximum subgroups each has been developed for isotypic $PrSe_2$ [2]. ZrSSi crystallizes in space group $P4/nmm$ (No. 129). In a first *translationengleich* step of index two the symmetry is reduced to the orthorhombic subgroup $Pmmn$ (No. 59). In this $t2$ step the fourfold rotation along [001] is lost. The next symmetry reduction results in monoclinic space group $P2_1/m$ (No. 11). In the course of this $t2$ descent the twofold rotation along [001] is also destroyed. By doubling the a axis, a *klassengleich* symmetry reduction of index two, the actual space group $P12_1/a1$ (No. 14) is reached. During both $t2$ steps twinning is likely to occur and accordingly the investigated crystal turned out to be a fourfold twin. The twinning matrices resemble the loss of fourfold (and twofold) rotation axes along [001], see table 1. Pseudomerohedral twinning of α-LnX_2 structures has frequently been found [2, 6, 8d–f]. Due to the monoclinic angle β being close to 90° and the particular relation of the lattice parameters $a \approx c \approx 2\,b$ combined with reflection conditions which are inconsistent with space group symmetry, the diffraction pattern of a (multiply) twinned α-LnX_2 crystal could be mistaken for pseudocubic. This may be the explanation for *Webb* and *Hall's* interpretation of the diffraction images [13]. The cell parameter 7.882(3) Å of their pseusocubic phase agrees well with the cell parameter a of our investigated crystal.

Table 3: GdS_2. Selected interatomic distances (d in Å).

Gd – S1$^{\#4}$	2.778(1)	Gd – S2$^{\#5}$	2.791(1)
Gd – S1$^{\#2}$	2.785(1)	Gd – S2$^{\#3}$	2.948(1)
Gd – S1	2.831(1)	Gd – S2$^{\#2}$	3.024(1)
Gd – S1$^{\#1}$	2.925(1)	Gd – S2$^{\#5}$	3.072(1)
Gd – S1$^{\#3}$	3.031(1)		
S2 – S2$^{\#8}$	2.140(1)	S2 – S2$^{\#9}$	2.960(1)
S2 – S2$^{\#7}$	2.960(1)	S2 – S2$^{\#10}$	3.186(2)

Symmetry codes:
#1 $-x+1/2,y-1/2,-z+1$; #2 $-x+1/2,y+1/2,-z+1$; #3 $-x,-y+1,-z+1$;
#4 $-x,-y+2,-z+1$; #5 $x,y,z+1$; #6 $x,y+1,z+1$; #7 $-x+1/2,y+1/2,-z$;
#8 $-x,-y+1,-z$; #9 $-x+1/2,y-1/2,-z$; #10 $-x,-y,-z$

Thermodynamic Studies

The thermal behaviour of solid GdS_2 is characterized by the incongruent thermal decomposition towards solid compounds richer in gadolinium ($GdS_{1.9}$(s), $GdS_{1.85}$(s), etc.) and gaseous sulfur (mainly S_2(g)). In order to understand the decomposition mechanism and to evaluate the concrete decomposition conditions (temperature and pressure) several methods of investigation have been applied: By thermodynamic modeling of the heterogeneous equilibria the existence ranges (lg(p/bar) vs. T^{-1}) of all gadolinium sulfides $GdS_{2-\delta}$ were estimated (Figure 2). Based on this information the phase barogram of the system Gd/S has been established. The decomposition reactions were experimentally verified by total pressure measurement (Figure 3) and thermal analysis in combination with mass spectrometry (TG/MS).

Including the known phases of gadolinium polysulfides $GdS_{2-\delta}$, the decomposition of GdS_2 proceeds step-wise (5) – (8) in analogy to the incongruent decomposition of PrS_2 [12a]:

$$20\ GdS_{2.00}(s) \rightarrow 20\ GdS_{1.90}(s) + S_2(g) \quad (5),$$

$$40\ GdS_{1.90}(s) \rightarrow 40\ GdS_{1.85}(s) + S_2(g) \quad (6),$$

$$25\ GdS_{1.85}(s) \rightarrow 25\ GdS_{1.77}(s) + S_2(g) \quad (7),$$

$$7.41\ GdS_{1.77}(s) \rightarrow 7.41\ GdS_{1.50}(s) + S_2(g) \quad (8).$$

The thermodynamic standard data $\Delta H^0_{298}(GdS_x)$ and $S^0_{298}(GdS_x)$ of the gadolinium sulfides were taken from the literature for GdS and $GdS_{1.5}$ (see table 4; [17]). Unknown data for the polysulfides $GdS_{2-\delta}$ were estimated in comparison with the data of the praseodymium sulfides [12a]. Applying *Kirchhoff's* laws and *Hess'* law for the thermodynamic data of the phases in reactions (5 – 8) yielded $\Delta H^0_R(GdS_x)$ and $\Delta S^0_R(GdS_x)$ for the respective polysulfides. Finally the phase barogram of the system Gd/S was developed by calculating the decomposition functions $\lg(p(S_2)/\text{bar}) = f(T^{-1})$ (9) of gadolinium sulfides:

$$\lg(p(S_2)/\text{bar}) = -\frac{\Delta H^0_R(GdS_x)}{2.303 \cdot R} \cdot \frac{1}{T} + \frac{\Delta S^0_R(GdS_x)}{2.303 \cdot R} \qquad (9),$$

with R being the universal gas constant.

The lines depicted in the barogram (Figure 2) mark the coexistence of adjacent phases, the areas in between the equilibrium lines correspondingly characterize the existence ranges of the individual phases. Following this way, the conditions for the synthesis of single phases GdS_x can be deduced: The composition GdS_2 is thermodynamically stable at a given temperature with a pressure above the solid line. At $T = 570$ K the decomposition pressure $p(S_2)$ is lower than 10^{-3} bar (100 Pa) and the compound is stable at ambient conditions. A rise in temperature causes an increased decomposition pressure: $p \approx 1$ bar (100 kPa) at $T = 870$ K and $p \approx 10^3$ bar (0.1 GPa) at $T = 1270$ K. Thus, at higher reaction temperatures pressure has to be applied to counterbalance the decomposition pressure in order to obtain GdS_2 under equilibrium conditions.

Table 4: Thermodynamic data for of phases in the system Gd–S.

Phase	ΔH^0_{298} / kJ·mol^{-1}	S^0_{298} / J·mol^{-1}·K^{-1}	C_p / J·mol^{-1}·K^{-1}	Reference
Gd	0	67.9	32.8	[17]
GdS	–460.0	77.4	58.0	[17]
Gd_2S_3	–1205.0	187.0	141.0	[17]
$GdS_{1.77}$	–612.0	101.6	77.3	
$GdS_{1.85}$	–612.9	104.2	79.3	[17]
$GdS_{1.90}$	–613.4	105.8	80.5	
$GdS_{2.00}$	–613.9	108.8	83.0	
$S_{2(g)}$	0	32.0	25.0	[17]

Insert Figure 2 here

The phase barogram of GdS_2 has been experimentally verified using total pressure measurements with a *Bourdon* manometer (see experimental section). The decomposition reaction starts at temperatures above 570 K with a pressure of 10^{-3} bar (100 Pa), and follows the course of the equilibrium line (Figure 3). With an average sample mass of about 75 mg, the decomposition of GdS_2 is completed at about 670 K and a drift towards the decomposition line of $GdS_{1.9}$ is observed The course of measured decomposition pressures of GdS_2 and $GdS_{1.9}$ confirms the equilibrium conditions calculated in the phase barogram. As a conclusion, GdS_2 is stable at temperatures below 670 K under its own decomposition pressure, while the phase is unstable at temperatures above 670 K without compensation of the sulfur pressure.

Insert Figure 3 here

Finally, the decomposition of GdS_2 was studied at ambient pressure using thermogravimetry in an argon atmosphere. In accordance with the phase barogram, the thermal degradation of GdS_2 starts at $T \approx 470$ K and proceeds via four distinct steps, namely $GdS_{1.9}$, $GdS_{1.85}$, and $GdS_{1.77}$, towards Gd_2S_3. The constant final mass is reached at $T \approx 1020$ K; the solid product was identified by powder X-ray diffraction as a mixture of *A*-type Gd_2S_3 [18a] and *C*-type Gd_2S_3 [18b]. The gaseous decomposition products were analyzed by mass spectrometry: S_2 ($m/z = 64$) was identified as the main species. At lower temperatures the species $S_8(g)$, $S_6(g)$ and $S_4(g)$ were detected in minor amounts as well. Nevertheless the general decomposition mechanism of GdS_2 and $GdS_{2-\delta}$ according the equilibrium reactions (5 – 8) is confirmed.

The release of sulfur has only consequences for the planar chalcogen layers of the polysulfide. In GdS_2 the planar sulfide layers consists of S_2^{2-} dumbbells only while in $GdS_{1.9}$ dimeric S_2^{2-} anions, single S^{2-} anions and vacancies can be found in the layers [3]. The structure of $GdS_{1.85}$ is not yet known, it might either adopt the modulated $PrSe_{1.85}$ type [7] or a defect variant of the Gd_8Se_{15} structure, a 24-fold superstructure of the ZrSSi type [5]. The higher chalcogen deficiency is reflected in a higher amount of vacancies and single X^{2-} anions in the respective chalcogen layers in both structure patterns. The formation of chalcogen deficient polychalcogenides by depletion of sulfur comes to an end with $GdS_{1.77}$ before the ordinary sulfide Gd_2S_3 is formed. No meaningful structure model has been established for $LnX_{1.77}$ compounds yet although indications for the existence of phases of this approximate composition were found during several tensimetric studies [4, 12].

Physical Properties

The temperature dependence of the resistivity $\rho(T)$ could be followed down to 63 K where the resistance reached the upper limit of our experimental setup. The decrease in direction of increasing temperatures (Figure 4) indicates that GdS_2 is semiconducting. A lower estimate of 0.36 eV for the fundamental gap at room temperature may be obtained from the temperature dependence of $\rho(T)$. The high resistivity of approximately 0.13 Ωm at 300 K indicates that the polycrystalline sample material has only a small concentration of point defects. This finding and the semiconducting properties of GdS_2 indicate a valence compound in which the electrons of the anionic partial structure are located in bonds or free electron pairs as reflected by the description $[Gd^{3+}S^{2-}]_2[S_2^{2-}]$ with completely filled valence shells of the sulfur ions.

Insert Figure 4 here

The magnetic susceptibility $\chi = M/H$ of GdS_2 is strongly temperature dependant. The plot of the reciprocal susceptibility as a function of temperature (Figure 4) follows the *Curie-Weiss* law except for the lowest temperatures. From a fit for $T > 20$ K ($\mu_0 H = 0.1$ T data) an effective magnetic moment μ_{eff} of 7.92 μ_B and a paramagnetic *Weiss* temperature $\theta_P = -7.9$ K is calculated, the latter indicating antiferromagnetic interactions. The Gd^{3+} ion is, thanks to its half-filled 4*f* shell, a magnetic species without orbital moment ($L = 0$) and $S = 7/2$. The highly degenerate $^8S_{7/2}$ ground state is therefore not split by crystal fields and the value of the effective moment of the free ion of 7.94 μ_B agrees excellently with our observation. A cusp in $\chi(T)$ (see upper inset of Figure 5) observed at $T_N = 7.7(1)$ K (in $\mu_0 H =$ 0.01 T) marks the long-range antiferromagnetic ordering of the Gd^{3+} magnetic moments. An isothermal magnetization curve $M(H)$ well below T_N (1.8 K) shows a broad metamagnetic transition between fields of roughly 1 and 2 T. This transition is more clearly seen in a plot of $M(H)/H$ (see lower inset of Fig. 5). The transition has no hysteresis in field and indicates a discontinuity in the gradual turning of the magnetic moment toward fully ferromagnetic ordering. Full alignment of the gadolinium spins (7 μ_B) is not achieved in our maximum field $M(7\text{ T}) = 5.7\ \mu_B$.

Insert Figure 5 here

Conclusions

Gadolinium disulfide was obtained by high-pressure synthesis using different starting materials. GdS_2 adopts the monoclinic $CeSe_2$ type, a twofold superstructure of the ZrSSi type. GdS_2 is a paramagnetic semiconductor containing Gd^{3+} and exhibits antiferromagnetic order at $T_N = 7.7(1)$ K. The formation of this disulfide is achieved by counterbalancing its decomposition pressure of, e.g., $p \approx 10^3$ bar (0.1 GPa) at $T = 1270$ K. A synthesis of GdS_2 at ambient pressure thus fails either because of insufficient reactivity at lower temperatures (say below ≈ 850 K) or because the decomposition pressure is exceeded at elevated temperatures. It can be assumed that the syntheses of further, yet unknown rare-earth metal polysulfides under high-pressure conditions will be possible. The exploration of appropriate reaction conditions, especially for crystal growth, remains, however, still a challenge.

Experimental Section

Preparation and sample handling was performed under argon atmosphere in glove boxes (MBraun, $H_2O < 1$ ppm, $O_2 < 1$ ppm).

Gd_2S_3 was synthesized from a mixture of gadolinium (99.9 %, Treibacher) and sulfur (99.95 %, Alfa Aesar) in a molar ratio of 2 : 3 (10). The elements were filled in silica ampoules with glassy carbon crucibles which were sealed under dynamic vacuum ($p < 10^{-4}$ mbar). The ampoules were placed in a muffle furnace and heated to 1273 K in 24 h. After annealing at this temperature for 72 h the ampoules were cooled to 298 K in 24 h.

$$2\ Gd + {}^3/_2\ S_2 \rightarrow Gd_2S_3 \qquad (10)$$

The sesquisulfide was obtained as a mixture of the *A*-type (space group *Pnma*, [18a]) and *C*-type (defect Th_3O_4 type, $I\bar{4}3d$, [18b]) under these conditions.

For gadolinium polysulfide $GdS_{1.9}$ a solid state metathesis reaction was used [3], see equation (11). $GdCl_3$ (99.9 %, Strem) and Na_2S_2 were mixed and filled in silica ampoules with glassy carbon crucibles. After sealing under dynamic vacuum the ampoules were annealed 9 days at 1023 K and afterwards cooled to room temperature with a rate of 3 K/h.

$$2\ GdCl_3 + 3\ Na_2S_2 \rightarrow 2\ GdS_{1.9} + 6\ NaCl + 2.2\ S \qquad (11)$$

The excessive sulfur was eliminated by sublimation (623 K → 298 K) in a horizontal tube furnace. The sodium chloride which is formed during the reaction acts as flux medium; it was removed with a mixture of water and ethanol (1 : 1).

High-pressure syntheses were performed with a 1000 t hydraulic press (Fa. Voggenreiter) at 8(0.8) GPa and temperatures between 293(15) K and 1373(69) K. For force redistribution and pressure generation a *Walker*-type module was used with MgO (doped with 5% Cr_2O_3) octahedra of edge length 18 mm [19]. Starting materials were filled under argon into crucibles machined of hexagonal boron nitride. Stepped graphite tubes were used for heating [20]. No reaction between starting material or products and crucible material has been observed.

X-Ray diffraction experiments on powder samples were performed in transmission arrangements on a Huber Image Plate system G670 with Co $K\alpha_1$ radiation. The program package *WinXPow* was applied for the interpretation of the powder diffractograms [21]. Single crystal experiments were performed on a Bruker Kappa CCD diffractometer with Mo $K\alpha$ radiation using the software package *SAINT* [22]. Structure images have been realized with *DIAMOND* [23].

Chemical analysis for hydrogen, nitrogen and oxygen was performed with the carrier gas hot extraction method on a LECO TCH 600. For EDXS analysis the sample were embedded with Technovit 550, ground with silicon carbide paper and polished with diamond suspensions. The EDXS analysis was performed with a Philips XL30 with LaB_6 cathode and a Si(Li) detector.

Thermogravimetric measurements were carried out with corundum crucibles in an analyzer STA 409 CD from NETZSCH skimmer-coupled to a mass spectrometer (Quadstar 422, Pfeiffer). Measurements were performed in the temperature range from $T = 298$ K to 1470 K with a heating rate of 10 K·min^{-1} in argon atmosphere. Buoyancy was corrected by measuring the empty crucible before the experiment. The particular decomposition temperature was determined at the onset of the corresponding weight loss.

Total pressure measurements were carried out in a *Bourdon* manometer of silica glass [24]. Measuring points have been collected every 20 K in the temperature range from $T = 520$ K to 820 K.

Estimation of standard data: The standard enthalpies of formation of phases $GdS_{2-\delta}$ have been estimated based on the values of analogous praseodymium sulfides. As for all unknown standard entropies of formation and functions of heat capacity presented in this work, approximations of S^0_{298} and $C_p(T)$ have

been performed according to the *Neumann-Kopp* rule as the stoichiometric sum of the particular values of Gd_2S_3 and S.

Physical properties of GdS_2 were measured on a polycrystalline piece of the same batch from which the crystal for structure determination and material for TG/MS analysis was taken. The electrical resistance was measured by the four-point method using direct current in the temperature range 4 – 320 K. The magnetization was determined in magnetic fields $\mu_0 H$ between 0.01 T and 7 T and temperatures between 1.8 K and 400 K in a SQUID magnetometer (MPMS XL-7, Quantum Design).

Acknowledgments

The authors thank Susann Leipe for supporting high-pressure synthesis, Dr. Stefan Hoffmann and Susann Scharsach for the TG/MS measurements, Gudrun Kadner for the measurement of vapor pressure, and Dr. Marcus Schmidt as well as Prof. Dr. Juri Grin for helpful discussions. The competence groups Analytics and Structure at the MPI CPfS are gratefully acknowledged as well as financial support by the Deutsche Forschungsgemeinschaft.

[1] W. Biltz, *Berichte d. Dt. Chem. Gesellschaft* **1908**, *41*, 3341–3350.

[2] Th. Doert, Chr. Graf, *Z. Anorg. Allg. Chem.* **2005**, *631*, 1101–1106.

[3] Th. Doert, Chr. Graf, P. Lauxmann, Th. Schleid, *Z. Anorg. Allg. Chem.* **2007**, *633*, 2719–2724.

[4] Th. Doert, Chr. Graf, P. Schmidt, I. G. Vasilieva, P. Simon, W. Carrillo-Cabrera; *J. Solid State Chem.* **2007**, *180*, 496–509.

[5] Th. Doert, E. Dashjav, B. P. T. Fokwa, *Z. Anorg. Allg. Chem.* **2007**, *633*, 261–273.

[6] Th. Schleid, P. Lauxmann, Chr. Graf, Chr. Bartsch, Th. Doert, *Z. Naturforsch.* **2009**, *64b,* 189–196.

[7] Chr. Graf, Th. Doert, *Z. Kristallogr.* **2009**, *224*, 568–579.

[8] a) J. P. Marçon, R. Pascard, *C.R. Acad. Sci. Paris, Ser. C* **1968**, *266*, 270–272; b) S. Bénazeth, D. Carré, M. Guittard, J, Flahaut, *C.R. Acad. Sci. Paris, Ser. C* **1975**, *280*, 1021–1024; c) S. Bénazeth, M. Guittard, J, Flahaut, *J. Solid State Chem.* **1981**, *37*, 44–48; d) S. Bénazeth, D. Carré, P. Laruelle, *Acta Crystallogr.* **1982**, *B38*, 33–37; e) S. Bénazeth, D. Carré, P. Laruelle, *Acta Crystallogr.* **1982**, *B38*, 37–39; f) R. Tamazyan, H. Arnold, V. N. Molchanov, G. M. Kuzmicheva, I. G. Vasilieva, *Z. Kristallogr.* **2000**, *215*, 272–277.

[9] a) Y. Yanagisawa, S. Kume, *Mater. Res. Bull.* **1973**, *8*, 1241–1246; b) Y. Yanagisawa, F. Kanamaru, S. Kume, *Acta Crystallogr.* **1979**, *B35*, 137–139; c) Y. Yanagisawa, S. Kume, *Mater. Res. Bull.* **1986**, *21*, 379–385.

[10] a) R. Tamazyan, H. Arnold, V. N. Molchanov, G. M. Kuzmicheva, I. G. Vasilieva, *Z. Kristallogr*. **2000**, *215*, 346–351; b) P. Plambeck-Fischer, W. Abriel, W. Urland, *J. Solid State Chem*. **1989**, *78*, 164–169; c) W. Urland, P. Plambeck-Fischer, M. Grupe, *Z. Naturforsch. B*. **1989**, *44*, 261–264; d) M. Gruppe, W. Urland, *J. Less Common Met*. **1991**, *170*, 271–275; e) E. Dashjav, Th. Doert, P. Böttcher, H. Mattausch, O. Oeckler, *Z. Kristallogr. NCS* **2000**, *215*, 337–338.

[11] a) A. van der Lee, L. M. Hoistad, M. Evain, B. J. Foran, S. Lee, *Chem. Mater*. **1997** *9*, 218–226.; b) R. Tamazyan, S. van Smaalen, I. G. Vasilyeva, H. Arnold, *Acta Crystallogr.* **2003** *B59*, 709–719.

[12] a) Chr. Graf, P. Schmidt, Th. Doert, *unpublished results*; b) T. P. Chusova, L. N. Zelenina, I. G. Vasilyeva, Chr. Graf, Th. Doert, *J. Alloys Comp.* **2008** *452*, 94–98.

[13] a) A. W. Webb, H. T. Hall, *Inorg. Chem.* **1970**, *9*, 843–847; b) A. W. Webb, H. T. Hall, *Inorg. Chem.* **1970**, *9*, 1084–1090.

[14] a) O. Degtyareva, E. Gregoryanz, M. Somayazulu, P. Dera, H. K. Mao, R. J. Hemley, *Nat. Mater.* **2005**, *4*, 152–155; b) O. Degtyareva, E. R. Hernandez, J. Serrano, M. Somayazulu, H. K. Mao, E. Gregoryanz, R. J. Hemley, *J. Chem. Phys.*. **2007**, *126*, 084503

[15] *SADABS*, G. M. Sheldrick, University of Göttingen, Germany, **2004**.

[16] *JANA2006. The crystallographic computing system,* V. Petricek, M. Dusek, L. Palatinus, Institute of Physics, Praha, Czech Republic, **2009**.

[17] a) O. Knacke, K. Kubaschewski, K. Hesselmann, *Thermochemical Properties of Inorganic Substances*, Springer, Berlin, Heidelberg, New York, **1991**; b) K.C. Mills, *Thermodynamic Data for Inorganic Sulfides, Selenides and Tellurides*, Butterworths, London, **1974**; c) I. G. Vasilieva, *Neorg. Mater.* **1985**, *21*, 1043–1045.

[18] a) A. W. Sleight, C. T. Prewitt, *Inorg. Chem.* **1968**, *7*, 1090–1093; b) Th. Schleid, F. A. Weber, *Z. Anorg. Allg. Chem.* **1998**, *624*, 557–558.

[19] D. Walker, M. A. Carpenter, C. M. Hitch, *Am. Mineral*. **1990**, *75*, 1020–1028.

[20] M. J. Walter, Y. Thibault, K. Wei, R. W. Luth, *Can. J. Phys*. **1995**, *73*, 273–286.

[21] *WinXPow. Powder diffraction software,* Stoe & Cie., Darmstadt, Germany, **1999**.

[22] *SAINT.* Bruker AXS Inc.; Madison, Wisconsin, USA, **2008**.

[23] *DIAMOND 3*, *Crystal and molecular structure visualization,* Crystal Impact, GbR, Bonn, **2009**.

[24] H. Oppermann, O. Schneider, E. Wittig, *Chem. Techn.* **1966**, *18*, 433.

Received: ((will be filled in by the editorial staff))
Published online: ((will be filled in by the editorial staff))

Figure captions:

Figure 1: Crystal structure of GdS_2, central projection of the unit cell along [010] (left) and dumbbell pattern of disulfide anions (right); ellipsoids at a 99.9% probability level.

Figure 2: Phase barogram of the system Gd – S calculated according to equation (9) using the standard data of the polysulfide phases (table 4).

Figure 3: Measurement of the decomposition pressure of GdS_2 and $GdS_{1.85}$ [17] in comparison to calculation of the decomposition equilibria.

Figure 4: Electrical resisitivity $\rho(T)$ of polycrystalline GdS_2.

Figure 5: Reciprocal magnetic susceptibility $1/\chi$ of GdS_2 as function of temperature T in two different external fields $\mu_0 H$ (0.1 T and 1 T). Upper inset: magnetic susceptibility $\chi(T)$ for $\mu_0 H$ = 0.01 T at low temperatures. Lower inset: magnetic susceptibility χ as function of external field $\mu_0 H$ for T = 1.8 K. See text for discussion.

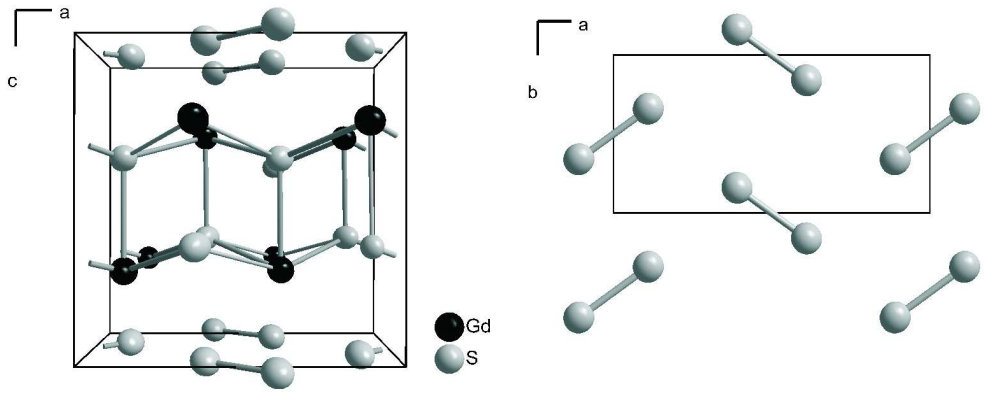

Figure 1: Crystal structure of GdS_2, central projection of the unit cell along [010] (left) and dumbbell pattern of disulfide anions (right); ellipsoids at a 99.9% probability level.
79x33mm (500 x 500 DPI)

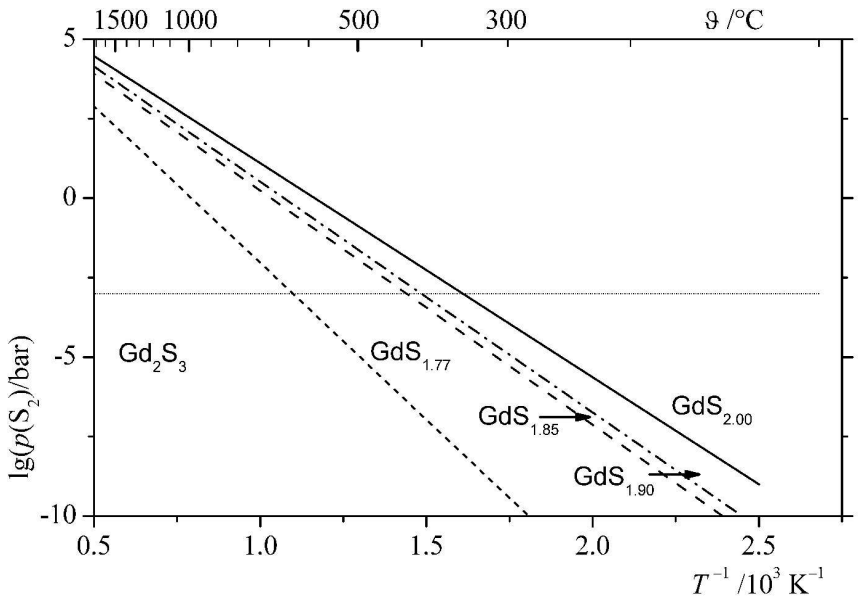

Figure 2: Phase barogram of the system Gd - S calculated according to equation (9) using the standard data of the polysulfide phases (table 4).
275x197mm (600 x 600 DPI)

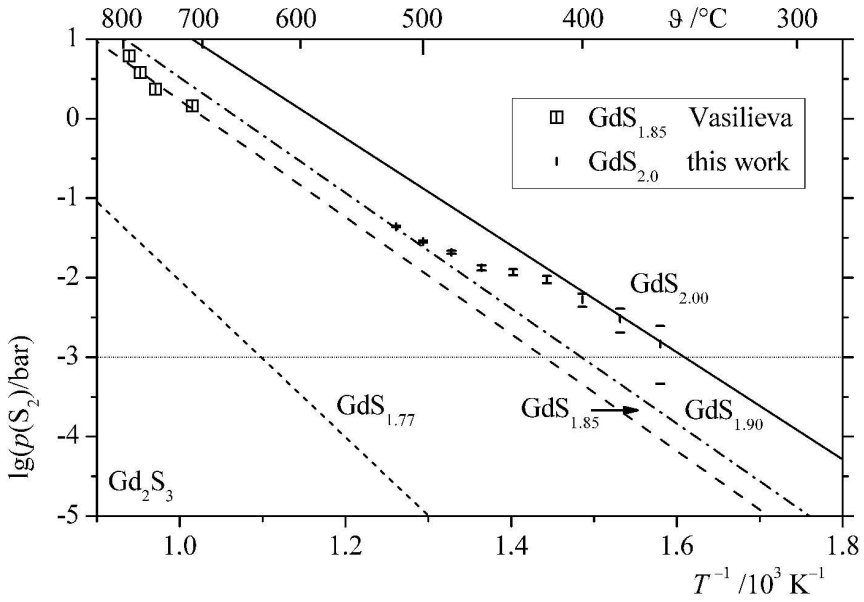

Figure 3: Measurement of the decomposition pressure of GdS_2 and $GdS_{1.85}$ [17] in comparison to calculation of the decomposition equilibria.
276x197mm (600 x 600 DPI)

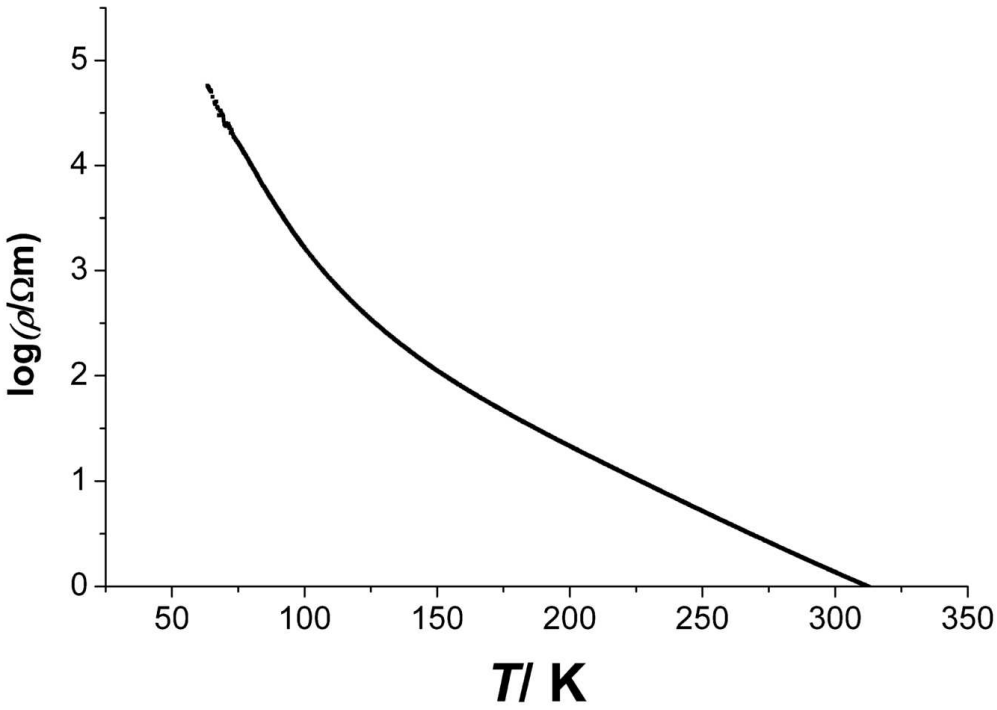

Figure 4: Electrical resisitivity ρ(*T*) of polycrystalline GdS_2.
56x40mm (600 x 600 DPI)

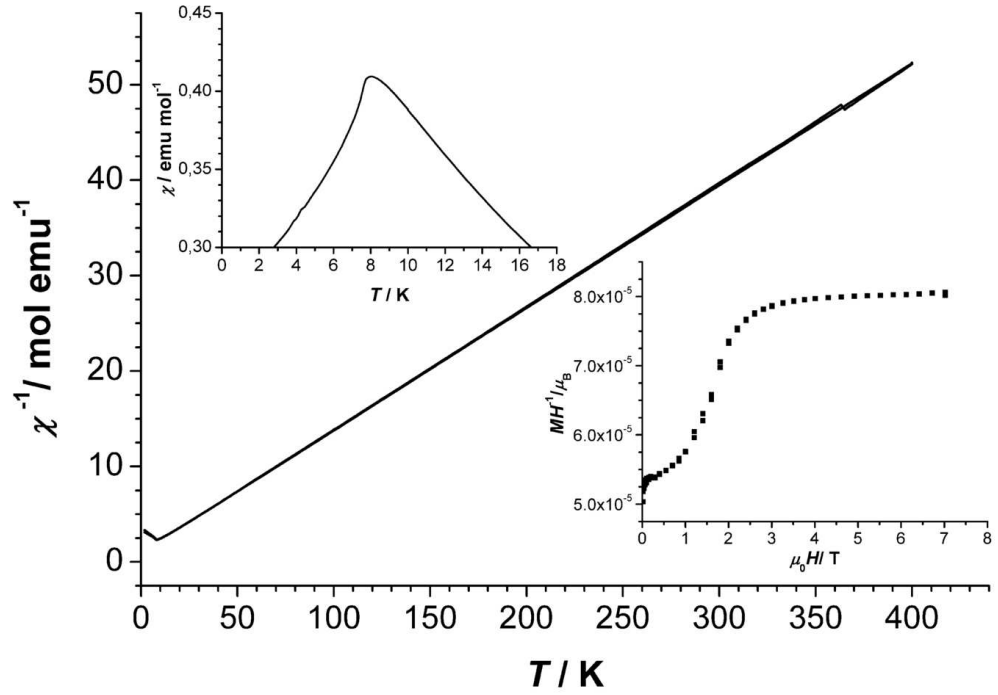

Figure 5: Reciprocal magnetic susceptibility $1/\chi$ of GdS_2 as function of temperature T in two different external fields $\mu_0 H$ (0.1 T and 1 T). Upper inset: magnetic susceptibility $\chi(T)$ for $\mu_0 H$ = 0.01 T at low temperatures. Lower inset: magnetic susceptibility χ as function of external field $\mu_0 H$ for T = 1.8 K. See text for discussion.
57x41mm (600 x 600 DPI)